Noninvasive Evaluation of Nonalcoholic Fatty Liver Disease (NAFLD) Using 1H and 23Na Magnetic Resonance Imaging and Spectroscopy in a Rat Model.

P. N. Hopewell[1,2], and N. Bansal[1]

[1]Department of Radiology, Indiana University School of Medicine, Indianapolis, IN, United States, [2]Weldon School of Biomedical Engineering, Purdue University, West Lafayette, IN, United States

Introduction

With increasing prevalence of the metabolic syndrome, non-alcoholic fatty liver disease (NAFLD) is now the most common chronic liver disease in humans [1]. Since symptoms caused by NAFLD appear late and current diagnosis requires biopsy, we hypothesized that magnetic resonance imaging/spectroscopy (MRI/S) techniques provide an early, noninvasive methodology to obtain a specific diagnosis. To test this hypothesis, a murine model of NAFLD, methionine- and choline-deficient diet (MCDD), was generated. MCDD increases the hepatic fat content by promoting peripheral lipolysis and hepatic uptake of fatty acids [2]. This study employed extensive lipid profiling via ^{1}H MRS to demonstrate temporal changes in lipid content, resolving 8 lipid resonance peaks plus water *in vivo*, with water- and fat-suppressed ^{1}H MRI. Single-quantum- (SQ) and multiple-quantum-(MQF) filtered ^{23}Na MRI were employed to evaluate cellular energy status as NAFLD progressed.

Methods

Wistar rats (~250 g) were placed on MCDD after baseline SQ and MQF ^{23}Na MRI and ^{1}H MRI/S were collected. Additional data were collected at 2, 5, and 10 weeks after initiating MCDD treatment. MR images were acquired with a Varian 9.4 Tesla, 31-cm horizontal bore system with a 12-cm gradient insert (maximum gradient strength = 38 G/cm). A 63-mm birdcage quadrature coil tuned to 400 MHz was used to collect all ^{1}H MRI/S data. Trans-axial images were collected using a spin-echo multislice sequence with respiratory gating. Three total scans were performed: CHESS suppression applied at 4.7 ppm (H_2O), CHESS suppression at 1.3 ppm $(CH_2)_n$, and without frequency suppression. The following imaging parameters were used: 1 s repetition time (TR), 11 ms echo time (TE), 256 x 128 data points over a 6 x 6 cm^2 field of view (FOV), 0.5 mm slice thickness, 0.1 mm slice gap, and 2 min imaging time. Fat-to-water ratios were determined from the signal intensity (SI) observed in the region of interest (ROI) corresponding to liver only. Spectroscopy data was collected using a localized adiabatic selective refocusing (LASER) sequence and respiratory gating. The spin-echo image without suppression was used as a scout image for voxel placement. The following imaging parameters were used: TR = 1 s, TE = 37.6 ms, 8 μL^3 voxel size, 128 data collections, 1000 spectral data points, and 2 min total collection time. 3D SQF trans-axial ^{23}Na MRI were obtained with a home-built loop-gap resonator tuned to 106 MHz. The SQF ^{23}Na MRI were collected using a gradient-echo (GE) imaging sequence and following imaging parameters: TR = 50 ms, TE = 4.5 ms, 64 x 64 x 16 data points over a FOV of 6 x 6 x 6 cm^3, and 10 min total imaging time. MQF ^{23}Na MRI employed the same parameters as used for SQ ^{23}Na MRI except TR = 100 ms, data size of 64 x 32 x 8, and 50 min total imaging time. A reference of 0.3% NaCl was used to normalize all data and to show that the MQF was functioning. Histologic samples were fixed in formalin and stained with H&E and trichrome stains.

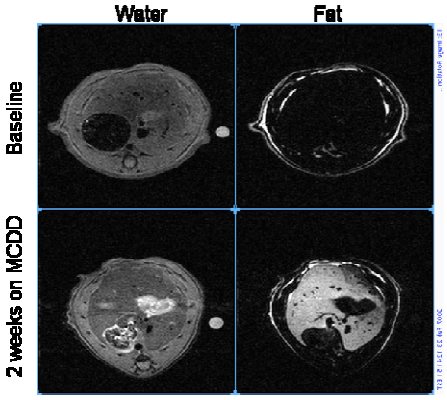

Fig. 1: Selected sections from transaxial ^{1}H water (left) and fat (right) MRI of rat liver before (top) and 2 weeks (bottom) after initiating MCD diet.

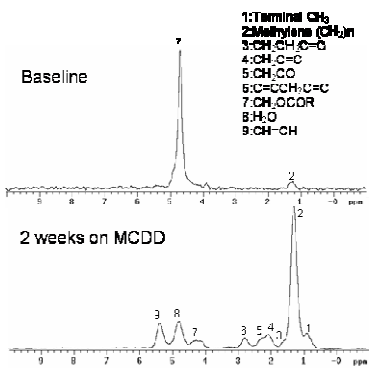

Fig. 2: Localized H spectra of rat liver before and 2 weeks after initiating MCD diet.

Results

Figures 1 and 2 are representative examples of water-suppressed and fat-suppressed ^{1}H MRI and ^{1}H MRS showing the difference between baseline and 2 weeks post-treatment with MCDD. After calculating the average SI of the ^{1}H images and normalizing the values to baseline, water/fat SI (8.2±0.78, $p<10^{-5}$) and the SI with water suppression (9.2±2.3, $p<0.001$) peak 2 weeks after starting MCDD. The fat suppression SI peaked at 10 weeks (1.6±0.60, $p<0.02$). LASER spectra showed marked changes in *in vivo* lipid resonances, with the $(CH_2)_n/H_2O$ reaching maximum at 5 weeks (7.3±0.38, $p<10^{-4}$), CH_2/CH_3 peaking at 2 weeks (12.4±3.1), and the unsaturated fatty acids/CH_2 reaching maximum at 10 weeks (0.23±0.014). Since baseline spectra only show H_2O and $(CH_2)_n$ peaks, p-values for ratios other than $(CH_2)_n/H_2O$ cannot be computed compared to baseline. Figure 3 shows representative SQF and MQF ^{23}Na images at baseline and 2 weeks post-MCDD treatment. Figure 4 shows the change in SQF and MQF SI throughout the study. Time points at week 5 and 10 show significant variations from baseline values (*$p<0.02$). Histological samples showed an increase in lipid concentration corresponding to the MRI/S and progressive development of fibrosis starting at week 5.

Discussion and Conclusions

Even though the water- and fat- suppressed MRI did not directly correlate temporally with the most dominant lipid peak, $(CH_2)_n$, the relative changes in other lipid peaks showed that the development of fatty liver to fibrosis is not merely a change in $(CH_2)_n/H_2O$, but also changes in different lipid moieties. Selective frequency suppression or excitation techniques are acceptable when the suppression or excitation pulse bandwidths are narrow enough not to interfere with the frequency of the peaks of interest in the Fourier domain. Yet when peaks of interest are near or within the suppression/excitation frequency, their signal will be lost or dampened when suppression is applied.

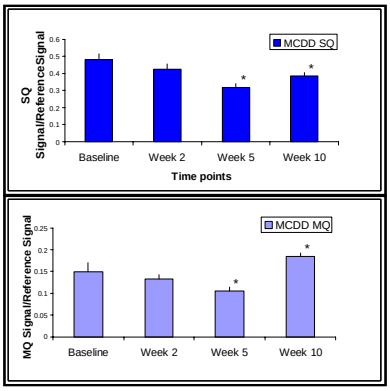

Fig. 3: SQ (top) and MQ (bottom) ^{23}Na MRI signal intensities for baseline data and weeks 2, 5, and 10 after initiating MCDD treatment. *$p<0.02$

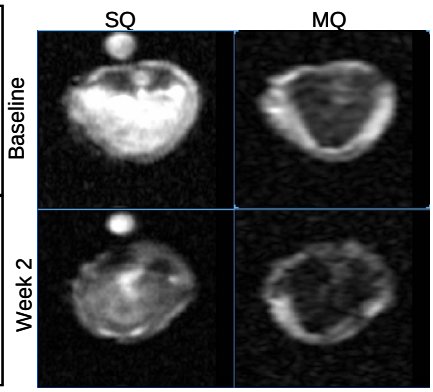

Fig. 4: ^{23}Na SQ (left) and MQ (right) filtered MRI of rat liver before (top) and 2 weeks (bottom) after MCDD.

The decrease in SQF and MQF filtered ^{23}Na MRI SI at week 2 and 5 is hypothesized to be due to Na^{+}'s insolubility in lipid, leading to a relative decrease in concentration. Yet as lipid content decreased by week 10, the SQF and MQF ^{23}Na MRI SI increased. This could be due to more Na^{+} being soluble as the lipid concentration decreases. An alternative theory suggests that increased collagen and macromolecule deposition associated with the fibrotic state creates an extracellular environment that makes MQ transitions possible. Intra- versus extracellular shift reagent studies and ^{31}P MRS are being performed to determine the underlying mechanism.

In conclusion, these data indicate our ability to profile different lipid resonances and provide support of our ability to detect and stage NAFLD using LASER ^{1}H MRS and SQF and MQF ^{23}Na MRI.

References

[1] Grattagliano, et al. Can Fam Physcian. 2007: 53:857-63

[2] Koteish A, et al. Best Pract Res Clin Gastroenterol. 2002: 6:679-90